High-Speed GaN-Based Blue Light-Emitting Diodes With Gallium-Doped ZnO Current Spreading Layer

Chien-Lan Liao, Yung-Fu Chang, Chong-Lung Ho, and Meng-Chyi Wu

***Abstract*—Conventional light-emitting diodes (LEDs) always pursue the high brightness required for solid-state lighting. However, they always exhibit very low frequency bandwidth of tens MHz. In this letter, we investigate the fabrication and characterization of high-speed GaN-based blue LEDs. The frequency response of LEDs is mainly limited by its diffusion capacitance and resistance, and the injected carriers in the active region of the device. Through appropriate device design, gallium-doped Zinc oxide film deposited by atomic layer deposition is used as the top contact layer with high lateral resistance to self-confine the current injection. In addition, a smaller bonding pad is used to reduce the RC time constant. Thus, the GaN-based blue LEDs with a 75-μm diameter exhibit a 3-dB modulation bandwidth of 225.4 MHz and a light output power of 1.6 mW at the current of 35 mA. Such LEDs can be applied to visible light communication in future.**

***Index Terms*—3-dB modulation bandwidth, atomic layer deposition (ALD), gallium-doped Zinc oxide (GZO), GaN, light-emitting diodes (LEDs).**

I. INTRODUCTION

RECENTLY, GaN and its alloys with InN and AlN has attracted much attention because of their suitability for use such as green-, blue-, and ultraviolet-light emitters as well as for applications in next generation lighting and high-power electronic devices [1], [2]. It is expected that the light-emitting diodes (LEDs) have lower driving voltage, lower power consumption, longer lifetime, smaller size, and cooler operation as compared with the conventional lighting sources. The use and development of high-efficiency light sources would decrease $>50\%$ of the worldwide lighting power consumption. Currently, highly efficient blue and green GaN-based LEDs have become commercially available. Now, it adds great importance to develop the high brightness and high-speed visible and white LEDs.

It is possible to fabricate white LEDs by mixing three primitive colors (RGB). As an application, visible light communication (VLC) is not only for illumination but also for data transmission communication [3], [4]. It is a kind of optical wireless communication that uses the visible white ray as the medium. This LED lighting has the characteristic of very quick response time (high 3-dB bandwidth) compared with the conventional light sources.

Sheu *et al.* used the textured InSnO/gallium-doped Zinc oxide (ITO/GZO) [5] or GZO [6] contact layer deposited by sputtering as the current-spreading layer to enhance light output power of GaN/InGaN LEDs as compared with the conventional LEDs with flat surface. Yen *et al.* reported the GZO films prepared by atomic layer deposition (ALD) as transparent conducting layer on GaN/InGaN LEDs to reduce the forward voltage and enhance the light output power [7]. However, the LEDs with the higher illumination power always lead to a lower modulation bandwidth of only tens MHz [8], [9]. Although there are literatures reported on the higher frequency response of 200–300 MHz for the GaN/InGaN LEDs, the LEDs had a smaller chip size or exhibited a lower light output power [3], [5], [10]. In this letter, we report on the fabrication of GaN-based blue LEDs with a GZO current spreading layer to exhibit a high electrical-to-optical (E–O) 3-dB bandwidth of 225.4 MHz and a high light output power of 1.6 mW at the bias current of 35 mA.

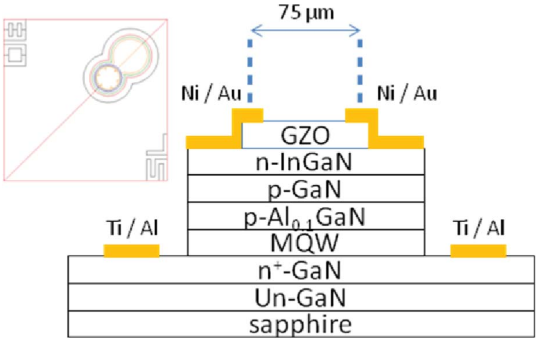

Fig. 1. Epitaxial structure for blue high-speed LED. Inset: designed mask after overlapping with five steps.

II. EXPERIMENT

High-speed LED structure employed in this letter is shown in Fig. 1. The LED wafers are grown by metal-organic chemical vapor deposition on sapphire substrates. Considering high response and high brightness, the layers consist of the following: 1) a 800-nm undoped GaN buffer layer; 2) a 3000-nm n^+-GaN confinement layer; 3) a multiple quantum well (MQW) active region, which consists of five 3-nm $In_xGa_{1-x}N$ quantum wells separated by four 14.4-nm GaN barrier layers; 4) a 20-nm p-$Al_{0.1}Ga_{0.9}N$ confinement layer; 5) a 560-nm p-GaN capping layer ($p \sim 5 \times 10^{17}$ cm^{-3}); 6) a very thin 1.4-nm n^+-InGaN (with in content of 0.12, $n^+ \sim 1.1 \times 10^{20}$ cm^{-3}) contact layer; and 7) a 250-nm GZO film deposited by ALD. For the ALD process, diethylzinc, triethylgallium, and water vapor (H_2O) are used as the precursors of Zn, Ga, and O, respectively. Precursors are pulsed one-by-one to separate the chemical reaction in every cycle into the reaction chamber at a deposition temperature of 325° [10].

After the epitaxial growth, the devices are fabricated using standard processing techniques, including sample cleaning,

---

Manuscript received February 4, 2013; accepted March 8, 2013. Date of publication March 28, 2013; date of current version April 22, 2013. The work was supported by the National Science Council under Grant 100-2221-E-007-084-MY3. The review of this letter was arranged by Editor J.-M. Liu.

The authors are with the Institute of Electronics Engineering, National Tsing Hua University, Hsinchu 30013, Taiwan (e-mail: mcwu@ee.nthu.edu.tw).

Color versions of one or more of the figures in this letter are available online at http://ieeexplore.ieee.org.

Digital Object Identifier 10.1109/LED.2013.2252457

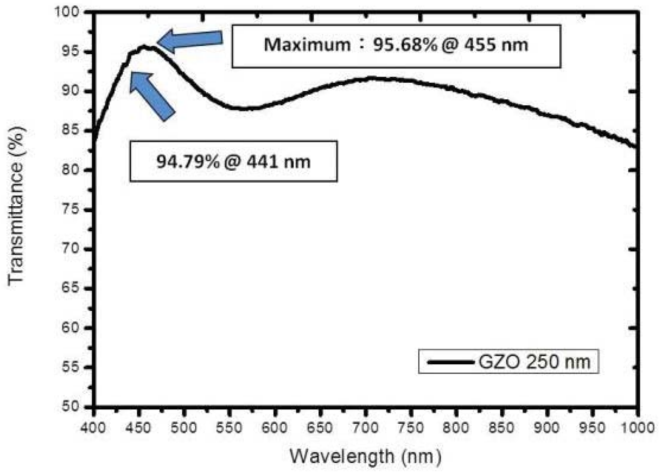

Fig. 2. Transmittance spectra of 250-nm thick as-grown GZO films deposited on sapphire substrates.

photolithography, metallization, lapping, polishing, describing, and bonding. As shown in Fig. 1, the light emitted out of the bottom electrode would not participate in the enhancement of external quantum efficiency. To avoid excessive lateral current spreading, we use the design of ring-shaped electrode contact. In addition, the GZO layer is overlapped with the ring-shaped electrode. In response to the high-frequency operation, the fabricated devices have a short diameter of current-confined aperture of 75 μm, a small diameter of bonding pad of 80 μm, and a chip size of 400 × 400 μm. The inset of Fig. 1 shows the designed mask after overlapping with five steps. The sapphire substrate is lapped and polished from 430 to 130 μm. Such a thinner substrate provides better heat dissipation at higher currents applied to the device for a long time.

III. RESULTS AND DISCUSSION

There are two core technologies in the concept of our design: 1) an ALD-deposited GZO film with low contact resistance is used as the top contact layer with high lateral resistance. Thus, the self-confined current injection structure is fabricated. It would enhance the injected current density and make the injected current uniformly distribute onto the GZO film, and 2) To reach smaller RC time constant, we not only designed smaller bonding pad but also used rapid thermal annealing process to repair the defects introduced from etching process and epitaxial defects of the active region. It is well-known that the frequency response of an LED is limited by its diffusion capacitance and resistance, and the injected carriers in the active region of devices. The minority carrier lifetime (τ_{tot}) is determined by radiative recombination lifetime (τ_r) and nonradiative recombination lifetime (τ_{r}) and nonradiative recombination lifetime (τ_{nr})

$$\frac{1}{\tau_{\text{tot}}} = \frac{1}{\tau_r} + \frac{1}{\tau_{\text{nr}}}.$$

It is not desired to shorten the nonradiative recombination lifetime, but preferable to shorten the radiative recombination lifetime. To achieve the current injection in a defined area, a technique of a ring-shaped electrode overlapping with GZO film is employed.

GZO recently become a very popular material as a transparent contact [11]–[13]. GZO is a wideband gap (for example) material and an n-type semiconducting oxides. Our previous results reveal that, the deposited GZO layers have a doping concentration of ~9.9×10^{20} cm^{-3}, low sheet resistance (~3.7×10^4 Ω-cm), and high transmittance (92.9%). It is expected that the current spreading would be well-performed in the GZO-covered active region. In this situation, we design an n-InGaN layer as the top layer, which also provides a good ohmic contact, as shown in Fig. 1.

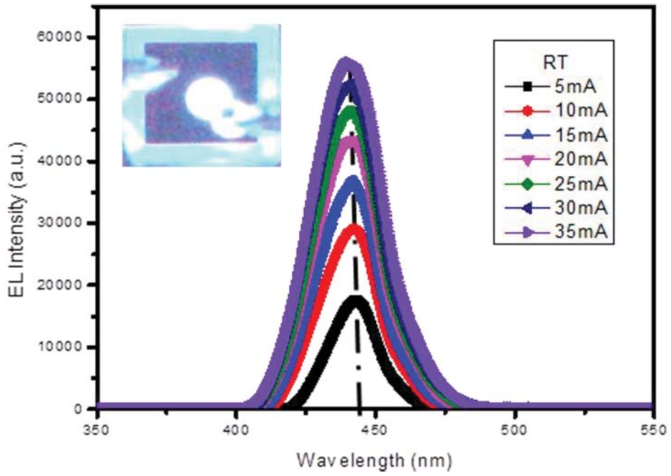

Fig. 3. Room-temperature EL spectra under various currents of LED with 75-μm-diameter active region. Inset: actual top-view image of emitting device.

Fig. 2 shows the transmittance spectra of the 250-nm thick as-grown GZO films deposited on sapphire substrates. The GZO film has the maximum transmittance of 95.7% at 455 nm and 94.8% at 441 nm. Based on the GZO films deposited onto the device, the optical transparency is still kept high. The current crowding problem is also alleviated because of the high sheet resistance of GZO film. Fig. 3 shows the room-temperature electroluminescence (EL) spectra under various currents of the LED with a 75-μm-diameter active region.

The actual top-view image of the emitting device is shown in the inset of Fig. 3. The measured peak wavelength λ_{peak} of the device is ~441 nm. With increasing the current, the λ_{peak} slightly shifts toward shorter wavelengths because of the quantum confined Stark effect (QCSE) occurred in the InGaN well in MQW region [14]. Piezoelectric fields are formed when the epitaxial layers are with different lattice constants; on the other hand, piezoelectric fields can be attributed to QCSE-created band bending in MQWs.

Fig. 4 shows the capacitance versus reverse bias (C-V) and current versus forward bias (I-V) for the LED device. The average capacitance values are only ~2 pF. The designed diameter of the bonding pad (80 μm) is smaller for the device because it can directly reduce the parasitic capacitance. The low dielectric coefficient oxide (SiO_2) under the bonding pad is used to reduce the bypass capacitor as well. Based on both the methods, the device would have a good capacitance performance. The LED exhibits the current-voltage (I-V) characteristics of a forward voltage of 4.9 V at 20 mA, a series resistance of 28 ω, and an ideality factor of 2.6 in the range of 2.0–2.4 V. The inset of Fig. 4 shows the image of the full structure observed by field-emission scanning electron microscopy (FE-SEM, JSM-7000F).

Fig. 5 shows the light output power as a function of forward current (L-I) measured at 300 K for the 441-nm high-speed LED. The L-I characteristic is measured by using

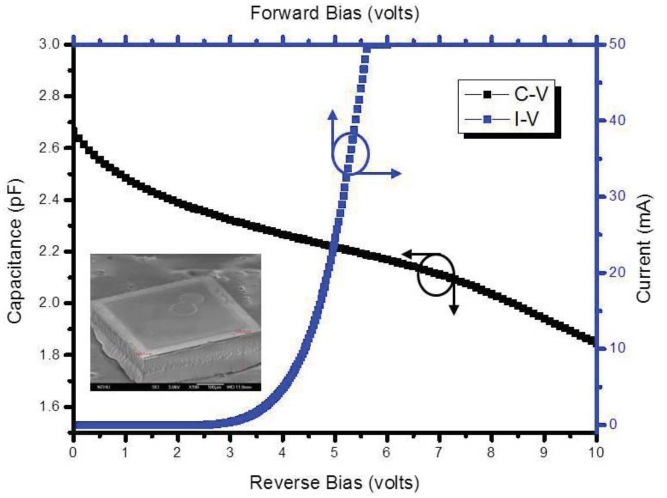

Fig. 4. Capacitance versus reverse bias (C-V) and current versus forward bias (I-V) for LED device. Inset: image of full structure tilted at 60° observed by FE-SEM.

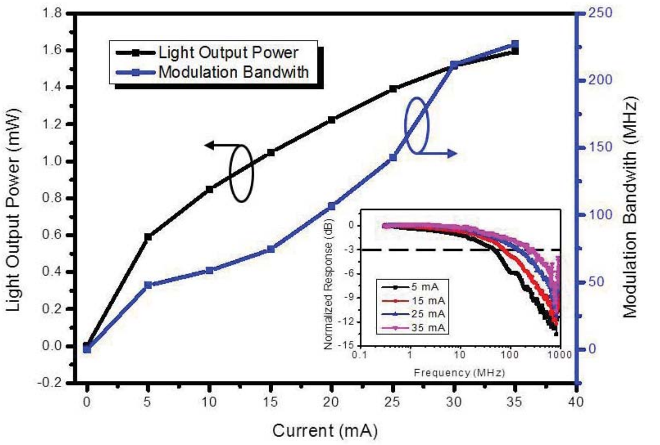

Fig. 5. Light output power and 3-dB frequency bandwidth ($f_{3\mathrm{dB}}$) as function of forward current measured at 300 K for 441-nm high-speed LED. Inset: spectra of 3-dB frequency bandwidth at various currents.

a large area detector which is installed in the integrated sphere. By calibrating the multiple scattering reflections, the LED reveals a light output power of 0.6, 1.1, 1.4, and 1.6 mW at the current of 5, 15, 25, and 35 mA, respectively. An increase of the injected current would raise the light output power because of the increase of radiative recombination of injected carriers. In addition, the thinner substrate could avoid the red shift, which may cause the degradation of light output power. The 3-dB frequency bandwidth ($f_{3\mathrm{dB}}$) as a function of forward current is also shown in Fig. 5. The 3-dB frequency bandwidth is defined as the frequency at which the output optical power received at a detector is reduced by 3 dB. The f3dB increases with driving current and achieves a maximum of 48.3, 74.6, 142.7, and 225.4 MHz at a current of 5, 15, 25, and 35 mA, respectively, for this LED with a 75-μm diameter, as shown in the inset of Fig. 5. The $f_{3\mathrm{dB}}$ of this device is much higher than that of the conventional LEDs owing to the above-mentioned concepts.

An optimum design of the confined region will increase the injected current density and 3-dB modulation bandwidth. However, it still exists a tradeoff. However, it cannot apply arbitrarily higher currents for the purpose to achieve higher frequencies or reduce the bonding pad area whatever we want. The LEDs are limited by thermal effect and carrier overflowing effect. This high-speed LED is required to be designed not only for illumination but also for communication in future.

IV. CONCLUSION

By an appropriate device structure design, we can improve the carrier injection density in the active region and avoid much of the lateral current spreading. It was demonstrated that the GaN-based blue LEDs with a 75-μm diameter exhibited a 3-dB frequency bandwidth of 225.4 MHz and a light output power of 1.6 mW at the current of 35 mA. Such LEDs can be applied to VLC in future.

REFERENCES

[1] C. T. Lee and C. Y. Chuang, “Light extraction enhancement of GaN-based flip-chip light-emitting diodes using diffused nanorod reflector,” *Appl. Phys. Exp.*, vol. 5, no. 11, pp. 112104–12104-3, Oct. 2012.

[2] L. W. Jang, J. W. Ju, D. W. Jeon, J. W. Park, A. Y. Polyakov, S. J. Lee, J. H. Baek, S. M. Lee, Y. H. Cho, and I. H. Lee, “Enhanced light output of InGaN/GaN blue light emitting diodes with Ag nano-particles embedded in nano-needle layer,” *Opt. Exp.*, vol. 20, no. 6, pp. 6036–6041, Mar. 2012.

[3] J. J. D. McKendry, R. P. Green, A. E. Kelly, Z. Gong, B. Guilhabert, D. Massoubre, E. D. Gu, and M. D. Dawson, “High-speed visible light communications using individual pixels in a micro light-emitting diode array,” *IEEE Photon. Technol. Lett.*, vol. 22, no. 18, pp. 1346–1348, Sep. 2010.

[4] J. J. D. McKendry, D. Massoubre, S. L. Zhang, B. R. Rae, R. P. Green, E. Gu, R. K. Henderson, A. E. Kelly, and M. D. Dawson, “Visible-light communications using a CMOS-controlled micro-light-emitting-diode array,” *J. Lightw. Technol.*, vol. 30, no. 1, pp. 61–67, Jan. 2012.

[5] J. K. Sheu, M. L. Lee, Y. S. Lu, and K. W. Shu, “Ga-doped ZnO transparent conductive oxide films applied to GaN-based light-emitting diodes for improving light extraction efficiency,” *IEEE J. Quantum Electron.*, vol. 44, no. 12, pp. 1211–1218, Dec. 2008.

[6] S. H. Tu, C. J. Lan, S. H. Wang, M. L. Lee, K. H. Chang, R. M. Lin, J. Y. Chang, and J. K. Sheu, “InGaN gallium nitride light-emitting diodes with reflective electrode pads and textured gallium-doped ZnO contact layer,” *Appl. Phys. Lett.*, vol. 96, no. 13, pp. 133504-1–133504-3, 2010.

[7] K. Y. Yen, C. H. Chiu, C. W. Li, C. H. Chou, P. S. Lin, T. P. Chen, T. Y. Lin, and J. R. Gong, “Performance of InGaN/GaN MQW LEDs using Ga-doped ZnO TCLs prepared by ALD,” *IEEE Photon. Technol. Lett.*, vol. 24, no. 23, pp. 2105–2108, Dec. 2012.

[8] M. Meier, S. Karg, and W. Riess, “Light-emitting diodes based on poly-p-phenylene-vinylene: II. Impedance spectroscopy,” *Appl. Phys. Lett.*, vol. 82, no. 4, pp. 1961–1966, May 2007.

[9] W. S. Wong, T. Sands, N. W. Cheung, M. Kneissl, D. P. Bour, P. Mei, L. T. Romano, and N. M. Johnson, “Fabrication of thin-film InGaN light-emitting diode membranes by laser lift-off,” *Appl. Phys. Lett.*, vol. 75, no. 10, pp. 1360–1362, Sep. 1999.

[10] J. W. Shi, J. K. Sheu, C. H. Chen, G. R. Lin, and W. C. Lai, “High-speed GaN-based green light-emitting diodes with partially n-doped active layers and current-confined apertures,” *IEEE Electron Device Lett.*, vol. 29, no. 2, pp. 158–160, Feb. 2009.

[11] K. Saito, Y. Hiratsuka, A. Omata, H. Makino, S. Kishimoto, T. Yamamoto, N. Horiuchi, and H. Hirayama, “Atomic layer deposition and characterization of Ga-doped ZnO thin films,” *Superlattices Microstruct.*, vol. 42, nos. 1–6, pp. 172–175, 2007.

[12] H. Y. Liu, X. Li, S. Liu, X. Ni, M. Wu, V. Avrutin, N. Izyumskaya, U. Ozgur, A. B. Yankovich, A. V. Kvit, P. M. Voyles, and H. Morkoc, “InGaN based light emitting diodes utilizing Ga doped ZnO as a highly transparent contact to p-GaN,” *Phys. Stat. Solidi C*, vol. 8, no. 5, pp. 1548–1551, Mar. 2011.

[13] W. C. Song, S. I. Kwon, G. S. Kang, J. H. Park, K. J. Yang, and D. G. Lim, “Characteristics of GZO films prepared by using a RF magnetron plasma at low temperature,” *J. Korean Phys. Soc.*, vol. 53, no. 5, pp. 2522–2526, Nov. 2008.

[14] T. Takeuchi, C. Wetzel, S. Yamaguchi, H. Sakai, H. Amano, I. Akasaki, Y. Kaneko, S. Nakagawa, Y. Yamaoka, and N. Yamada, “Determination of piezoelectric fields in strained GaInN quantum wells using the quantum-confined Stark effect,” *Appl. Phys. Lett.*, vol. 73, no. 12, pp. 1691–1693, Jul. 1998.